Microfluid Nanofluid (2008) 4:363–374
DOI 10.1007/s10404-007-0185-0

RESEARCH PAPER

Oscillatory Couette flow at arbitrary oscillation frequency over the whole range of the Knudsen number

Felix Sharipov · Denize Kalempa

Received: 1 April 2007 / Accepted: 22 May 2007 / Published online: 29 June 2007

Abstract The oscillatory Couette flow is important for further advancement of microengineering. In practice the size of the microfluidics can be so small that it can be compared with the molecular mean free path. Moreover, the oscillation frequency can be close to that of the intermolecular collisions. Under such conditions the problem must be solved on the kinetic level. In the present work, the oscillatory Couette flow is considered on the basis of the non-stationary kinetic equation. The solution to the problem is determined by two parameters: the Knudsen number and the ratio of collision frequency to oscillation frequency. The kinetic equation is solved by the discrete velocity method over the wide range of both parameters.

Keywords Microfluidics · Rarefied gas · Knudsen number · Oscillation speed parameter · Damping force

1 Introduction

Many microfluidics contain oscillating parts, which are subject to a damping force caused by a surrounding gas. To calculate such a force and other characteristics, such as velocity distribution around an oscillating part, usually the non-stationary Navier–Stokes equation is applied. However, this approach is justified under the following two conditions. First, the molecular mean free path must be significantly smaller than a characteristic size of the gas flow. Second, the molecular mean free time must be significantly smaller than a characteristic time of the gas flow. If at least one of these conditions is not satisfied then the problem must be solved on the basis of the kinetic equation.

The stationary Couette flow problem have been studied extensively by solving the time-independent Boltzmann kinetic equation and its models (see e.g. Cercignani and Pagani 1966; Gross and Ziering 1958; Loyalka et al. 1979; Marques et al. 2000; Sharipov et al. 2004; Siewert 2002; Sone et al. 1990; Willis 1962). As will be shown below such a solution can be applied at any gas rarefaction, but only to slowly oscillating surfaces. However, in microfluidics an oscillation can be so fast that the stationary solution is not valid anymore; but to calculate the damping force and the velocity distribution the time-dependent kinetic equation should be solved. In the open literature there are very few papers concerning time-dependent cases like the oscillatory Couette flow.

In our previous work (Sharipov and Kalempa 2007), we studied the time dependent behavior of gas flow in an infinite half-space caused by a flat plate oscillating in its own plane by considering a time periodic solution of the non-stationary kinetic equation. This solution can be applied to situations when the oscillating surface is so far from other surfaces that the distance between them is significantly larger than the mean free path. However, if this distance is comparable with the mean free path the time-dependent solution must take into account the presence of a fixed surface. Such a situation was considered in Hadjiconstantinou (2005) and Park et al. (2004), where the oscillatory Couette flow was studied by applying the direct simulation Monte Carlo method.

In the present work, we study the oscillatory Couette flow problem on the basis of the non-stationary kinetic equation. It is assumed that the oscillation is to be fully established through the gas flow and, consequently, the solution is harmonic with respect to the time.

F. Sharipov (✉) · D. Kalempa
Departamento de Física, Universidade Federal do Paraná,
Caixa Postal 19044, Curitiba 81531-990, Brazil
e-mail: sharipov@fisica.ufpr.br

2 Statement of the problem

We consider a monoatomic gas confined between two infinite plates parallel to the yz-plane. The plate placed at $x' = 0$ oscillates harmonically in the y-direction with frequency ω, while the other plate is fixed at $x' = L'$. The velocity of the oscillating plate can be represented as

$$U_w = \Re[U_{w0} \exp(-i\omega t')], \tag{1}$$

where $\Re$ denotes the real part of a complex expression and U_{w0} is the velocity amplitude of the oscillating plate, which is assumed to be very small when compared with the most probable molecular velocity v_0 of the gas flow, i.e.,

$$U_{w0} \ll v_0, \quad v_0 = \left(\frac{2kT}{m}\right)^{1/2}, \tag{2}$$

where m is the molecular mass, T is the gas temperature and k is the Boltzmann constant.

The oscillatory plate motion causes a gas flow in the y-direction characterized by the bulk velocity U_y and shear stress P_{xy}, which depend on the time harmonically as

$$U_y(t', x') = \Re\left[\tilde{U}_y(x') \exp(-i\omega t')\right], \tag{3}$$

$$P_{xy}(t', x') = \Re\left[\tilde{P}_{xy}(x') \exp(-i\omega t')\right], \tag{4}$$

where $\tilde{U}_y(x')$ and $\tilde{P}_{xy}(x')$ are complex functions completely determining the gas flow. If one needs to calculate the damping force one uses just the quantity $\tilde{P}_{xy}$ at $x' = 0$. If one is interested in the velocity distribution in the gas then one uses the quantity $\tilde{U}_y(x')$.

As has been mentioned above the problem under question is determined by the two parameters. The first is the gas rarefaction δ defined as

$$\delta = \frac{PL'}{\mu v_0} \sim \frac{1}{Kn}, \tag{5}$$

where P is the gas pressure, μ is the shear viscosity of the gas, and Kn is the Knudsen number. Since the quantity $\ell = \mu v_0/P$ is the equivalent mean free path, the rarefaction parameter δ characterizes the relation between the characteristic size L' and the mean free path ℓ, but it does not contain any information about the oscillation speed.

To characterize the oscillation speed the second parameter is necessary, which was introduced in Sharipov and Kalempa (2007), viz.

$$\theta = \frac{P}{\mu\omega}. \tag{6}$$

Since the quantity $\nu = P/\mu$ is the intermolecular collision frequency, the parameter θ relates this frequency to that of the oscillation ω. However, this parameter does not contain any information about the characteristic size L'.

Thus, one can change δ and maintain θ varying the distance L'. It is also possible to change θ and to maintain δ varying the frequency ω. In other words, the parameters δ and θ are independent.

Sometimes, see e.g., Park et al. (2004), to characterize the oscillation speed the Stokes number is used, which is defined as

$$\beta = \sqrt{\frac{\omega\varrho}{\mu}}L = \sqrt{\frac{2}{\theta}}\delta. \tag{7}$$

This criterion represents a balance between the unsteady and viscous effects. The limit $\beta \ll 1$ represents a stationary flow, while in the case $\beta \gg 1$ a solution is essentially different from the stationary one. However, the Stokes number does not represent a limit of applicability of the Navier–Stokes equation. In other papers (see e.g. Hadjiconstantinou 2005), the ballistic Stokes number defined as

$$S_b = \frac{\omega L'}{v_0} = \frac{\delta}{\theta} \tag{8}$$

is used. This parameter is useful to analyze a free molecular oscillating flows like that considered in Sharipov et al. (2002).

For our purpose it is more convenient to present the results in terms of the parameters δ and θ. Once these parameters are given then the Stokes number and the ballistic Stokes number are calculated by Eqs. (7) and (8), respectively.

Regarding the values of the rarefaction parameter δ we may distinguish the two limits. If it is large, i.e., $\delta \gg 1$, then the space between the plates is so large that it can be considered as infinite, i.e., we have the half-space limit. If the rarefaction parameter is small, i.e., $\delta \ll 1$, then the distance L' is so small that the molecules move between the plates without intermolecular collisions. This regime is called as collisionless or free-molecular.

Considering the value of the oscillation speed parameter θ the following limits are distinguished. Large values ($\theta \gg 1$) correspond to a low oscillation frequency, i.e., the quasi-stationary flow. If the parameter is small ($\theta \ll 1$) then very few collisions occur during one oscillation period. This is the high-speed oscillation regime.

If both parameters are large, i.e., $\delta \gg 1$ and $\theta \gg 1$, then both conditions of the Navier–Stokes applicability are satisfied. This regime is called as hydrodynamic. However, if at least one of these conditions is not satisfied, then the Navier–Stokes equation is not valid and the problem must be solved on the basis of the kinetic equation.

For convenience, the following dimensionless quantities are introduced

$$t = \omega t', \quad x = \frac{\omega}{v_0} x', \quad L = \frac{\omega}{v_0} L'. \tag{9}$$

$$u(x) = \frac{\tilde{U}_y(x)}{U_{w0}}, \quad \Pi(x) = \frac{\tilde{P}_{xy(x)}}{2P} \frac{v_0}{U_{w0}}. \tag{10}$$

Note, the dimensionless distance between the plates is related to the parameters δ and θ as $L = \delta/\theta$.

Since $u(x)$ and $\Pi(x)$ are complex quantities, they can be written as

$$u(x) = u_m(x) \exp\left[i\varphi_u(x)\right], \tag{11}$$

$$\Pi(x) = \Pi_m(x) \exp\left[i\varphi_P(x)\right], \tag{12}$$

where $u_m(x)$ and $\Pi_m(x)$ are the amplitudes of the bulk velocity and shear stress, respectively, and $\varphi_u(x)$ and $\varphi_P(x)$ are their phases.

We are going to calculate the quantities $u_m(x)$, $\Pi_m(x)$, $\varphi_u(x)$ and $\varphi_P(x)$ over the whole range of both rarefaction δ and oscillation speed θ parameters.

3 Hydrodynamic regime

The hydrodynamic regime is characterized by large values of both rarefaction and oscillation speed parameters, i.e., $\delta \to \infty$ and $\theta \to \infty$, In this limit the Stokes equation can be applied, which in a general form reads (Landau and Lifshitz 1989)

$$-\varrho \frac{\partial \mathbf{U}}{\partial t'} + \mu \Delta \mathbf{U} = \nabla P, \tag{13}$$

where ϱ is the mass density and P is the pressure. Then, with the help of Eqs. (3, 6, 9, 10) and taking into account that the pressure is constant the Stokes equation (13) is reduced to

$$2i\theta u + \frac{\mathrm{d}^2 u}{\mathrm{d}x^2} = 0, \tag{14}$$

where the notations introduced above have been used. If we assume the non-slip boundary conditions at both walls, i.e.,

$$u = \begin{cases} 1 & \text{at} \quad x = 0, \\ 0 & \text{at} \quad x = L, \end{cases} \tag{15}$$

then Eq. (14) has the following solution

$$u(x) = \frac{\sin\left[(1+i)\left(\frac{\delta}{\sqrt{\theta}} - \sqrt{\theta}x\right)\right]}{\sin\left[(1+i)\frac{\delta}{\sqrt{\theta}}\right]}, \tag{16}$$

and, consequently, the shear stress Π of the gas flow is given by

$$\Pi(x) = -\frac{1}{2\theta}\frac{\mathrm{d}u}{\mathrm{d}x} = \frac{(1+i)}{2\sqrt{\theta}} \frac{\cos\left[(1+i)\left(\frac{\delta}{\sqrt{\theta}} - \sqrt{\theta}x\right)\right]}{\sin\left[(1+i)\frac{\delta}{\sqrt{\theta}}\right]}. \tag{17}$$

For moderately large values of θ and δ the solution (16) is corrected by the slip boundary conditions (Sharipov and Seleznev 1998), i.e.,

$$u = \begin{cases} 1 + \frac{\sigma_P}{\theta}\frac{du}{dx} & \text{at} \quad x = 0, \\ -\frac{\sigma_P}{\theta}\frac{du}{dx}, & \text{at} \quad x = L, \end{cases} \tag{18}$$

where σ_P is the viscous slip coefficient. Note, that the large value of the parameter θ corresponds to the slow oscillation so that the slip conditions are the same as for a stationary flow. Then, the solution of Eq. (14) with the boundary conditions (18) reads

$$u(x) = \frac{\sin\left[(1+i)\left(\frac{\delta}{\sqrt{\theta}} - \sqrt{\theta}x\right)\right]}{\sin\left[(1+i)\frac{\delta}{\sqrt{\theta}}\right]} \frac{\left\{1 + (1+i)\frac{\sigma_P}{\sqrt{\theta}}\cot\left[(1+i)\left(\frac{\delta}{\sqrt{\theta}} - \sqrt{\theta}x\right)\right]\right\}}{\left\{1 - 2i\frac{\sigma_P^2}{\theta} + 2(1+i)\frac{\sigma_P}{\sqrt{\theta}}\cot\left[(1+i)\frac{\delta}{\sqrt{\theta}}\right]\right\}}. \tag{19}$$

Note, that this expression can be used with any slip coefficient σ_P obtained rigorously from the different kinetic equations (Siewert and Sharipov 2002), for different values of the accommodation coefficients (Sharipov 2003), and even for a mixture (Sharipov and Kalempa 2003). An expression similar to Eq. (19) was obtained in Park et al. (2004), where questionable slip boundary conditions were used.

The shear stress $\Pi(x)$ is obtained as

$$\Pi(x) = -\frac{1}{2\theta}\frac{\mathrm{d}u}{\mathrm{d}x} = \frac{(1+i)}{2\sqrt{\theta}} \frac{\cos\left[(1+i)\left(\frac{\delta}{\sqrt{\theta}} - \sqrt{\theta}x\right)\right]}{\sin\left[(1+i)\frac{\delta}{\sqrt{\theta}}\right]} \times \frac{1 - (1+i)\frac{\sigma_P}{\sqrt{\theta}}\tan\left[(1+i)\left(\frac{\delta}{\sqrt{\theta}} - \sqrt{\theta}x\right)\right]}{1 - 2i\frac{\sigma_P^2}{\theta} + 2(1+i)\frac{\sigma_P}{\sqrt{\theta}}\cot\left[(1+i)\frac{\delta}{\sqrt{\theta}}\right]}. \tag{20}$$

It should be noted that to obtain an analogous expression the authors of Park et al. (2004) used the concept of the effective viscosity, which is very vague and useless. If one calculates it from different kinds of flows, e.g., plane Couette flow, cylindrical Couette flow, plane Poiseuille flow, etc., one obtains different kinds of the effective viscosity expressions.

It is interesting to consider two limit situations. First, when $\sqrt{\theta} \gg \delta \gg 1$, i.e. the oscillation is very slow, then Eqs. (19) and (20) are expanded into the Taylor series with respect to the small parameter $\delta/\sqrt{\theta}$. Retaining just the main term in this expansion we obtain

$$u(x) = \left(1 - \frac{x}{L} + \frac{\sigma_P}{\delta}\right)\left(1 + \frac{2\sigma_P}{\delta}\right)^{-1}, \quad \text{at} \quad \sqrt{\theta} \gg \delta, \tag{21}$$

$$\Pi(x) = \frac{1}{2\delta}\left(1 + \frac{2\sigma_P}{\delta}\right)^{-1}, \quad \text{at} \quad \sqrt{\theta} \gg \delta, \tag{22}$$

that coincide with the stationary Couette flow in the slip flow regime, see Eq. (12) of Sharipov et al. (2004). The other situation is that $\delta \gg \sqrt{\theta} \gg 1$, i.e. the ratio $\sqrt{\theta}/\delta$ is the small parameter. If one expands the expressions (19) and (20) into the Taylor series with respect to the parameter $\sqrt{\theta}/\delta$ and retains the main term one obtains the expressions corresponding to those given for the semi-infinite space in Sharipov and Kalempa (2007)

$$u(x) = \exp\left[(i-1)\sqrt{\theta}x\right]\left[1 - (i-1)\frac{\sigma_P}{\sqrt{\theta}}\right]^{-1}, \quad \text{at} \quad \sqrt{\theta} << \delta, \tag{23}$$

$$\Pi(x) = \frac{1}{\sqrt{2\theta}}\exp\left[(i-1)\sqrt{\theta}x - i\frac{\pi}{4}\right]\left[1 - (i-1)\frac{\sigma_P}{\sqrt{\theta}}\right]^{-1}, \quad \text{at} \quad \sqrt{\theta} << \delta. \tag{24}$$

4 Kinetic equation

For arbitrary values of both oscillation speed θ and rarefaction δ parameters the problem must be solved on the level of the velocity distribution function $f(t', \boldsymbol{r}', \boldsymbol{v})$ which obeys the time-dependent Boltzmann equation. Here, $\boldsymbol{r}'$ and $\boldsymbol{v}$ are the position and molecular velocity vectors, respectively. For the problem in question the non-stationary Boltzmann equation reads

$$\frac{\partial f}{\partial t'} + v_x\frac{\partial f}{\partial x'} = Q(ff^*), \tag{25}$$

where $Q(ff^*)$ denotes the collision integral.

Table 1 Comparison of shear stress Π_m for the stationary Couette flow ($\theta = \infty$) obtained from the Boltzmann equation (BE) in Sone et al. (1990) and from the BGK model

δ	Π_m	
	BE	BGK
7.874	0.05075	0.05048
3.937	0.08460	0.08391
1.968	0.1272	0.1262
0.7874	0.1844	0.1838
0.3937	0.2194	0.2196
0.1968	0.2445	0.2452
0.07874	0.2645	0.2651
0.03937	0.2726	0.2730

Till now, a numerical solution to the Boltzmann equation with the exact collision integral is a very difficult task; that is why some simplified models of the integral $Q(ff^*)$ were proposed. Such model equations are the widely used tools in practical calculations. However, a correct model should be chosen for each specific problem. As was shown in Sharipov and Seleznev (1998), isothermal rarefied gas flows are well described by the model proposed by (BGK) Bhatnagar et al. (1954). To confirm this claim a comparison of the shear stress Π_m for the stationary Couette flow ($\theta = \infty$) obtained from the Boltzmann equation (Sone et al. 1990) with that calculated from the BGK model using the technique described in Sharipov et al. (2004) is performed in Table 1. The results of Sone et al. (1990) were recalculated in our notations. It can be seen that the disagreement between the two solutions does not exceed 1%. So, the BGK model provides reliable results over the whole range of the rarefaction parameter δ with a significantly less computational effort.

Thus, like our previous work (Sharipov and Kalempa 2007), here we apply the BGK model representing the collision integral as

$$Q(ff^*) = \frac{P}{\mu}(f^M - f), \tag{26}$$

where

$$f^M = n\left(\frac{m}{2\pi kT}\right)^{3/2}\exp\left\{-\frac{m[\boldsymbol{v} - \boldsymbol{U}(t', \boldsymbol{r}')]^2}{2kT}\right\}, \tag{27}$$

is the local Maxwellian function, n, T and $\boldsymbol{U}$ are number density, temperature and bulk velocity of the gas, respectively. Due to the condition (2), the density n and temperature T can be considered constant, while the bulk velocity $\boldsymbol{U}$ has only the y-component expressed in terms of the distribution function as

$$U_y(t',x') = \frac{1}{n}\int v_y f(t',x',\boldsymbol{v})\mathrm{d}\boldsymbol{v}. \tag{28}$$

The shear stress of the gas flow is calculated via the distribution function as

$$P_{xy}(t',x') = m\int v_x(v_y - U_y) f(t',x',\boldsymbol{v})\mathrm{d}\boldsymbol{v}. \tag{29}$$

The condition (2) allows us to linearize the kinetic equation by representing the distribution function as

$$f(t',x',\boldsymbol{v}) = \frac{n}{(\sqrt{\pi}v_0)^3}\mathrm{e}^{-c^2}\left[1 + h(t,x,\boldsymbol{c})\frac{U_{w0}}{v_0}\right], \tag{30}$$

where $h(t, x, \boldsymbol{c})$ is the perturbation function and $\boldsymbol{c} = \boldsymbol{v}/v_0$ is the dimensionless molecular velocity.

Substituting (30) into (25) with (26) the linearized BGK equation is obtained in its dimensionless form

$$\frac{\partial h}{\partial t} + c_x\frac{\partial h}{\partial x} = \theta[2c_y\Re(u) - h]. \tag{31}$$

If we introduce the complex distribution function $\tilde{h}$ so that

$$h(t,x,\boldsymbol{c}) = \Re\left[\tilde{h}(x,\boldsymbol{c})\mathrm{e}^{-it}\right]. \tag{32}$$

then Eq. (31) is written down as

$$(\theta - i)\tilde{h} + c_x\frac{\partial\tilde{h}}{\partial x} = 2\theta c_y u. \tag{33}$$

From Eqs. (3, 4, 11, 12, 28) and (29) we obtain

$$u(x) = \frac{1}{\pi^{3/2}}\int c_y\mathrm{e}^{-c^2}\tilde{h}(x,\boldsymbol{c})\mathrm{d}\boldsymbol{c}, \tag{34}$$

$$\Pi(x) = \frac{1}{\pi^{3/2}}\int c_x c_y\mathrm{e}^{-c^2}\tilde{h}(x,\boldsymbol{c})\mathrm{d}\boldsymbol{c}. \tag{35}$$

The diffuse scattering of gaseous particles on both plates is assumed, i.e.

$$\tilde{h} = \begin{cases} 2c_y & \text{at} \quad x = 0 \quad \text{and} \quad c_x > 0, \\ 0 & \text{at} \quad x = L \quad \text{and} \quad c_x < 0. \end{cases} \tag{36}$$

In order to eliminate the variables c_y and c_z a new perturbation function is introduced

$$\Phi(x,c_x) = \frac{1}{\pi}\int c_y\exp\left(-c_y^2 - c_z^2\right)\tilde{h}(x,\boldsymbol{c})\mathrm{d}c_y\mathrm{d}c_z. \tag{37}$$

Multiplying Eq. (33) by $c_y\exp(-c_y^2-c_z^2)/\pi$ and integrating it with respect to c_y and c_z we obtain

$$(\theta - i)\Phi + c_x\frac{\partial\Phi}{\partial x} = \theta u. \tag{38}$$

The boundary conditions (36) are written in terms of the new function Φ as

$$\Phi = \begin{cases} 1 & \text{at} \quad x = 0 \quad \text{and} \quad c_x > 0, \\ 0 & \text{at} \quad x = L \quad \text{and} \quad c_x < 0. \end{cases} \tag{39}$$

The moments defined in (34) and (35) are expressed via the new perturbation function as

$$u(x) = \frac{1}{\sqrt{\pi}}\int \exp\left(-c_x^2\right)\Phi(x,c_x)\mathrm{d}c_x, \tag{40}$$

$$\Pi(x) = \frac{1}{\sqrt{\pi}}\int c_x\exp\left(-c_x^2\right)\Phi(x,c_x)\mathrm{d}c_x. \tag{41}$$

If we multiply Eq. (38) by $\exp[(\theta–i)x/c_x]$ and integrate it with respect to x, then taking into account the boundary conditions (39) we obtain

$$\Phi(x,c_x) = \exp\left[-(\theta-i)\frac{x}{c_x}\right] + \frac{\theta}{c_x}\int_0^x u(\xi)\exp\left[(\theta-i)\frac{\xi - x}{c_x}\right]\mathrm{d}\xi \quad \text{at} \quad c_x > 0, \tag{42}$$

$$\Phi(x,c_x) = -\frac{\theta}{c_x}\int_x^L u(\xi)\exp\left[(\theta - i)\frac{\xi - x}{c_x}\right]\mathrm{d}\xi \quad \text{at} \quad c_x < 0. \tag{43}$$

5 Collisionless flow

Consider a situation when the rarefaction parameter δ tends to zero, while the oscillation speed parameter θ is fixed and arbitrary. It is possible when the pressure is fixed, but the distance between the plates L' decreases. In this case the integration interval in Eqs. (42) and (43) will decrease because it is always smaller than the dimensionless distance L, i.e., the integrals will vanish at $L \to 0$. Since $x \le L$, then x tends to zero at $L \to 0$, i.e., the first term in the right hand side tends to unity. Then, Eqs. (42) and (43) are reduced to

$$\Phi(x,c_x) = \begin{cases} 1 & \text{at} \quad c_x > 0, \\ 0 & \text{at} \quad c_x < 0. \end{cases} \tag{44}$$

Substituting this solution into the definitions (40) and (41) we obtain

$$u(x) = \frac{1}{2}, \quad \Pi(x) = \frac{1}{2\sqrt{\pi}} \quad \text{at} \quad \delta = 0. \tag{45}$$

Physically, this result means that in the free molecular regime $\delta = 0$ the stationary solution can be used for any value of the oscillation speed parameter θ.

6 High-speed oscillation

Now consider the solution corresponding to the high-speed oscillation, i.e., when θ tends to zero while the rarefaction parameter δ is arbitrary. In this situation Eq. (38) is reduced to

$$-i\Phi + c_x \frac{\partial \Phi}{\partial x} = 0, \tag{46}$$

which satisfies the boundary conditions (39). Integrating (46) with respect to the coordinate x the analytical solution is obtained as

$$\Phi(x, c_x) = \begin{cases} \exp\left(i\frac{x}{c_x}\right) & \text{at} \quad c_x > 0, \\ 0 & \text{at} \quad c_x < 0. \end{cases} \tag{47}$$

The bulk velocity and shear stress are obtained by substituting this solution into Eqs. (40) and (41)

$$u(x) = \frac{1}{\sqrt{\pi}} I_0(-ix), \quad \Pi(x) = \frac{1}{\sqrt{\pi}} I_1(-ix) \quad \text{at} \quad \theta = 0, \tag{48}$$

where the special functions $I_n(z)$ are defined as (Abramowitz and Stegun 1972)

$$I_n(z) = \int_0^\infty c^n \exp\left(-c^2 - \frac{z}{c}\right) \mathrm{d}c. \tag{49}$$

The same expressions were obtained in our previous work (Sharipov and Kalempa 2007) considering the semi-infinite space. At the oscillating plate $x = 0$ the expressions (48) take the forms

$$u = \frac{1}{2}, \quad \Pi = \frac{1}{2\sqrt{\pi}} \quad \text{at } x = 0 \text{ and } \theta = 0, \tag{50}$$

i.e., the bulk velocity and the shear stress have the same values as that in the free-molecular regime ($\delta = 0$). The unique difference is that the quantities u and Π vary in the space in the high-speed regime ($\theta = 0$), while they are constant in the free molecular regime ($\delta = 0$).

7 Transitional regime

Two methods of solution of Eq. (38), viz. integro-moments and discrete velocities, are described in our previous work (Sharipov and Kalempa 2007). The first method works without the discretization of the velocity space, but it requires a large computer memory. The second method is based on the discretization of the molecular velocity space. However, it is necessary to consider a great number of nodes for the velocity because of the oscillatory behavior of the perturbation function. Furthermore, the convergence rate of the iteration procedure is very low when the parameters δ and θ are large.

In the present work, the discrete velocity method was improved so that the number of nodes in the velocity space was reduced using the split idea given Naris and Valougeorgis (2005) and the convergence acceleration was implemented following the algorithm described in Valougeorgis and Naris (2003). Since the details of the method are described in Sharipov and Kalempa (2007), here just its modifications will be given.

To reduce the number of the velocity nodes the perturbation function Φ is split into two parts as

$$\Phi = \tilde{\Phi} + \Phi_0, \tag{51}$$

where Φ_0 satisfies the following equation

$$(\theta - i)\Phi_0 + c_x \frac{\partial \Phi_0}{\partial x} = 0 \tag{52}$$

with the boundary conditions

$$\Phi_0 = \begin{cases} 1 & \text{at} \quad x = 0 \quad \text{and} \quad c_x > 0, \\ 0 & \text{at} \quad x = L \quad \text{and} \quad c_x < 0. \end{cases} \tag{53}$$

Eq. (52) has the following analytical solution

$$\Phi_0(x, c_x) = \begin{cases} \exp\left[-(\theta - i)\frac{x}{c_x}\right] & \text{at} \quad c_x > 0, \\ 0 & \text{at} \quad c_x < 0. \end{cases} \tag{54}$$

Substituting (51) into Eq. (38) the following equation for $\tilde{\Phi}$ is obtained

$$(\theta - i)\tilde{\Phi} + c_x \frac{\partial \tilde{\Phi}}{\partial x} = \theta u, \tag{55}$$

which satisfies the boundary condition

$$\tilde{\Phi} = \begin{cases} 0 & \text{at} \quad x = 0 \quad \text{and} \quad c_x > 0, \\ 0 & \text{at} \quad x = L \quad \text{and} \quad c_x < 0. \end{cases} \tag{56}$$

The moments $u(x)$ and $\Pi(x)$ are also decomposed into two parts as

$$u(x) = \tilde{u}(x) + u_0(x), \tag{57}$$

$$\Pi(x) = \tilde{\Pi}(x) + \Pi_0(x), \tag{58}$$

where

$$\tilde{u}(x) = \frac{1}{\sqrt{\pi}} \int \exp\left(-c_x^2\right) \tilde{\Phi}(x, c_x) \mathrm{d}c_x, \tag{59}$$

$$\tilde{\Pi}(x) = \frac{1}{\sqrt{\pi}} \int c_x \exp\left(-c_x^2\right) \tilde{\Phi}(x, c_x) \mathrm{d}c_x, \tag{60}$$

$$u_0(x) = \frac{1}{\sqrt{\pi}} \int \exp\left(-c_x^2\right) \Phi_0(x, c_x) \mathrm{d}c_x = \frac{1}{\sqrt{\pi}} I_0[(\theta - i)x], \tag{61}$$

$$\Pi_0(x) = \frac{1}{\sqrt{\pi}} \int c_x \exp\left(-c_x^2\right) \Phi_0(x, c_x) \mathrm{d}c_x = \frac{1}{\sqrt{\pi}} I_1[(\theta - i)x]. \tag{62}$$

Using such a split the oscillatory behavior was taken into account by the known function Φ_0, while the unknown function $\tilde{\Phi}$ is quite smoother than the initial function Φ. Then, the kinetic equation (55) is solved by exactly the same method as that described Sharipov and Kalempa (2007).

As has been mentioned above, when the parameters δ and θ are large the iteration convergence is very slow, i.e., the number of iterations drastically increases by increasing both parameters. In order to reduce the number of iterations the algorithm proposed in Valougeorgis and Naris (2003) is used. Let us introduce the Hermite moments defined as

$$F_n(x) = \frac{1}{\sqrt{\pi}} \int H_n(c_x) \exp\left(-c_x^2\right) \tilde{\Phi}(x, c_x) \mathrm{d}c_x, \tag{63}$$

where the functions $H_n(c_x)$ denote the nth order Hermite polynomial. Multiplying Eq. (55) by $\exp\left(-c_x^2\right)/\sqrt{\pi}$ and taking the first three Hermite moments we obtained the following accelerated synthetic equations

$$\frac{\mathrm{d}F_1}{\mathrm{d}x} = 2iF_0 + 2\theta u_0, \tag{64}$$

$$\frac{\mathrm{d}F_0}{\mathrm{d}x} + (\theta - i)F_1 = -\frac{1}{2}\frac{\mathrm{d}F_2}{\mathrm{d}x}, \tag{65}$$

where u_0 is given by (61). Taking into account that $F_0 = \tilde{u}$ and combining Eqs. (64) and (65) we obtain the following second order differential equation

$$\frac{\mathrm{d}^2\tilde{u}}{\mathrm{d}x^2} + 2(1 + i\theta)\tilde{u} = -2\theta(\theta - i)u_0 - \frac{1}{2}\frac{\mathrm{d}^2F_2}{\mathrm{d}x^2}. \tag{66}$$

In the beginning of iterations the bulk velocity $\tilde{u}$ is assumed to be equal to some arbitrary value, say zero. Then each iteration consists of the following steps:

(1) Kinetic equation (55) is solved to obtain the perturbation function $\tilde{\Phi}(x, c_x)$.
(2) The Hermit moment $F_2(x)$ is calculated by Eq. (63).
(3) The differential equation (66) is solved to obtain the moment $\tilde{u}$.
(4) The convergence is checked comparing $\tilde{u}$ in two successive iterations. If the convergence is not reached the next iteration is done beginning from step (i) using $\tilde{u}(x)$ obtained in the current iteration.

The iteration process stops when a convergence criterion is fulfilled.

8 Results and discussion

The numerical calculations were carried out over the wide range of the parameters δ and θ with the numerical error less than 0.1%. The accuracy was estimated by varying the number of nodes in both physical N_x and velocity N_c spaces. An analysis of the numerical data for different grids in the physical and velocity spaces showed that the values N_x = 10,000 and N_c = 400 provide the accuracy 0.1%.

The amplitude Π_m of the shear stress on both plates is presented in Table 2. In the previous work (Sharipov and Kalempa 2007) the penetration depth λ, which is defined as the distance x where the velocity amplitude decays up to 1% of that of the plate, was calculated. Its values are given in Table 2 together with the corresponding values of θ. Since the stationary plate is located at $L = \delta/\theta$ there is no sense in carrying out the calculations for $L > \lambda$, i.e., for $\delta > \lambda\theta$, because a further increase of the rarefaction parameter δ does not change the characteristics on the oscillating plate, while near the fixed plate the gas state becomes equilibrium.

In the last row of Table 2 the shear stress Π_m obtained from the non-stationary Navier–Stokes equation under the conditions $\delta \to \infty$, i.e. the solution Eq. (24) with σ_P = 1.016, is shown. In the 10th and 11th columns of Table 2 the shear stress calculated by Eq. (20) assuming θ = 50 and σ_P = 1.016 is given. This value of the slip coefficient σ_P was obtained in several papers reviewed in Sharipov and Seleznev (1998). A comparison of the data given in the last row and in the 10th and 11th columns with those obtained from the kinetic equation shows the range of applicability of the hydrodynamic equations with the slip boundary condition.

In the 12th column of Table 2 the shear stress corresponding to the stationary Couette flow, i.e. $\theta = \infty$, is given. These values were obtained from the stationary BGK equation by the same methodology as that used in Sharipov et al. (2004) for a mixture. Some of these data can be found in Cercignani and Pagani (1966) and Loyalka et al. (1979). A comparison of the non-stationary results with those obtained for the stationary flow will indicate the range of the applicability of the time-independent solution. In the 13th

Table 2 Amplitude of shear stress Π_m versus δ and θ at $x = 0$ and at $x = L$

δ	Π_m											
	$\theta = 0.1$		$\theta = 1$		$\theta = 10$		$\theta = 50$		Eq. (20) at $\theta = 50$		$\theta = \infty$	
	$\lambda = 7.5355$		$\lambda = 3.6010$		$\lambda = 1.3080$		$\lambda = 0.6210$					
	$x = 0$	$x = L$	$x = 0$	$x = L$	$x = 0$	$x = L$	$x = 0$	$x = L$	$x = 0$	$x = L$	Kin.eq (Cercignani and Pagani 1966; Loyalka et al. 1979; Sharipov et al. 2004)	Eq. (22)
0.	0.2821	0.2821	0.2821	0.2821	0.2821	0.2821	0.2821	0.2821	0.2461	0.2461	0.2821	0.2461
0.01	0.2801	0.2754	0.2797	0.2796	0.2797	0.2797	0.2797	0.2797	0.2449	0.2449	0.2797	0.2449
0.05	0.2788	0.2351	0.2714	0.2697	0.2709	0.2708	0.2708	0.2708	0.2402	0.2402	0.2708	0.2402
0.1	0.2813	0.1819	0.2634	0.2580	0.2612	0.2611	0.2612	0.2612	0.2345	0.2345	0.2612	0.2345
0.5	0.2819	0.0383	0.2521	0.1797	0.2093	0.2078	0.2084	0.2083	0.1975	0.1975	0.2083	0.1975
1	0.2819	0.0073	0.2665	0.1114	0.1741	0.1679	0.1697	0.1694	0.1651	0.1649	0.1695	0.1649
2	0.2819	0.0005	0.2696	0.0419	0.1465	0.1196	0.1262	0.1249	0.1250	0.1238	0.1252	0.1240
4	0.2819	0.0000	0.2688	0.0059	0.1531	0.0654	0.0888	0.0821	0.0885	0.0821	0.0830	0.0829
6	–	–	0.2688	0.0007	0.1622	0.0345	0.0774	0.0600	0.0772	0.0602	0.0623	0.0623
8	–	–	–	–	0.1632	0.0178	0.0770	0.5868	0.0768	0.0460	0.0498	0.0498
10	–	–	–	–	0.1627	0.0091	0.0803	0.0351	0.0803	0.0354	0.0416	0.0416
15	–	–	–	–	0.1625	0.0017	0.0865	0.0177	0.0867	0.0181	0.0294	0.0294
20	–	–	–	–	0.1625	0.0003	0.0870	0.0087	0.0871	0.0089	0.0227	0.0227
30	–	–	–	–	–	–	0.0866	0.0021	0.0867	0.0022	0.0156	0.0156
40	–	–	–	–	–	–	0.0866	0.0005	0.0868	0.0005	0.0119	0.0119
50	–	–	–	–	–	–	0.0866	0.0001	0.0868	0.0001	0.0096	0.0096
Eq. (24)	0.4220	0	0.3132	0	0.1644	0	0.0868	0				

column of Table 2 the shear stress obtained from the stationary Navier–Stokes equation ($\theta \to \infty$) with the slip boundary condition, i.e. the solution (22), is presented.

The shear stress phase φ_P is given in Table 3. In the 10th and 11th columns the phase calculated from Eq. (20) assuming $\theta = 50$ and $\sigma_P = 1.016$ is presented. In the last row of Table 3 the phase obtained from Eq. (24) is shown.

From the data showed in Tables 2 and 3 we conclude that

(1) The solution (20) based on the Navier–Stokes equation (14) with the slip boundary condition (18) is in agreement with the numerical solution of the kinetic equation if both conditions $\delta \gg 1$ and $\theta \gg 1$ are satisfied. In other words, if at least one of the two parameters δ and θ is not large the Navier–Stokes equation cannot be applied.

(2) The shear stress $\Pi_m(x)$ at the oscillating plate tends to its free molecular value $1/(2\sqrt{\pi})$ if at least one of the two conditions $\delta \to 0$ or $\theta \to 0$ is satisfied. In this sense, the regime can be called as free-molecular if $\delta = 0$ or $\theta = 0$.

(3) At any fixed value of the rarefaction parameter $\delta > 0$ the shear stress $\Pi_m(0)$ at the oscillating plate decreases by increasing the oscillation speed parameter θ, while the shear stress $\Pi_m(L)$ at the fixed plate increases.

(4) For a fixed value of oscillation parameter θ the amplitude $\Pi_m(0)$ at the oscillating surface has a non-monotonical dependence on rarefaction parameter δ, i.e. there is a minimum at the transition value of θ. To see better this minimum the shear stress is plotted versus δ/θ in Fig. 1. It can be seen that the shear stress Π_m undergoes a minimum in the interval $0.1\theta < \delta < \theta$. Then, a constant value of Π_m is established by further increasing the rarefaction parameter δ. The velocity amplitude u_m plotted in Fig. 2 has a maximum in the same interval of δ.

(5) The phase φ_P on the oscillating plate is always negative and tends to zero in the free-molecular regime ($\delta = 0$).

(6) The phase φ_P decreases by increasing the rarefaction parameter δ when the oscillation speed parameter θ is fixed, i.e. for large values of δ the shear stress becomes later when compared with the plate velocity phase.

Figures 3, 4, 5 show the dependence of the amplitude Π_m and phase φ_P on the dimensionless distance x/L. It can be seen that the behavior of the shear stress Π_m changes qualitatively by increasing of the rarefaction parameter δ,

Table 3 Phase of shear stress φ_P versus δ and θ at $x = 0$ and at $x = L$

δ	φ_P									
	$\theta = 0.1$		$\theta = 1$		$\theta = 10$		$\theta = 50$		Eq. (20) at $\theta = 50$	
	$x = 0$	$x = L$	$x = 0$	$x = L$	$x = 0$	$x = L$	$x = 0$	$x = L$	$x = 0$	$x = L$
0.01	–0.0025	0.1647	–0.0004	0.0173	0.0000	0.0017	0.0000	0.0003	–0.0002	0.0002
0.05	–0.0192	0.7026	–0.0072	0.0831	–0.0008	0.0084	–0.0002	0.0017	–0.0010	0.0010
0.1	–0.0248	1.2514	–0.0222	0.1608	–0.0026	0.0165	–0.0005	0.0033	–0.0021	0.0021
0.5	–0.0190	4.2781	–0.1590	0.7137	–0.0381	0.0812	–0.0077	0.0163	–0.0128	0.0125
1	–0.0188	6.9678	–0.1868	1.3051	–0.1158	0.1719	–0.0244	0.0346	–0.0314	0.0292
2	–0.0188	11.188	–0.1660	2.2782	–0.3124	0.3936	–0.0783	0.0805	–0.0864	0.0740
4	–0.0188	17.957	–0.1662	3.7228	–0.5199	0.9562	–0.2496	0.2114	–0.2577	0.2050
6	–	–	–0.1662	4.6309	–0.5226	1.5723	–0.4446	0.3921	–0.4538	0.3869
8	–	–	–	–	–0.5082	2.1837	–0.5868	0.6157	–0.5976	0.6123
10	–	–	–	–	–0.5053	2.7873	–0.6567	0.8712	–0.6680	0.8701
15	–	–	–	–	–0.5063	4.3073	–0.6686	1.5716	–0.6792	1.5778
20	–	–	–	–	–0.5063	5.8146	–0.6516	2.2796	–0.6614	2.2929
30	–	–	–	–	–	–	–0.6504	3.6806	–0.6603	3.7072
40	–	–	–	–	–	–	–0.6504	5.0813	–0.6604	5.1214
50	–	–	–	–	–	–	–0.6504	6.4821	–0.6604	6.5356
Eq. (24)	–0.1339	–	–0.3186	–	–0.5469	–	–0.6604	–		

i.e. the variation of Π_m is small for $\delta = 0.1$, while for $\delta = 10$ it sharply decays near the oscillating surface. The phase φ_P changes just quantitatively by increasing the rarefaction parameter δ.

The velocity amplitudes $u_m(x)$ and phases φ_u are given in Figs. 6, 7 and 8 as functions of the dimensionless coordinate x/L. The behavior of the velocity is similar to that of the shear stress.

Additional calculations were carried out to perform a comparison with data obtained in (Park et al. 2004). The results of the present work are shown by the lines in Figs. 9 and 10, while the data of Park et al. (2004) are given by the symbols. From these Figures we can see that for some values of δ and θ the results obtained in both works are in a fine agreement with each other, while for other values, viz. $\delta = 0.3545$, $\theta = 0.2513$; $\delta = 0.1772$, $\theta = 0.0628$; and $\delta = 0.3545$, $\theta = 0.0402$, there is a discrepancy. Since there is no any tendency in the disagreement we cannot explain its reason.

9 Conclusion

The oscillating Couette flow was calculated over the whole range of the rarefaction δ and oscillation speed θ parameters. The analytical expressions of the bulk

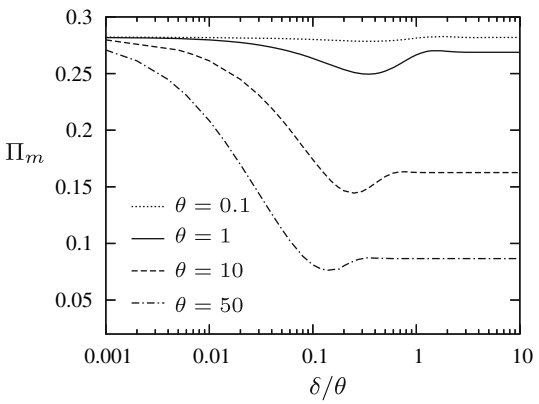

Fig. 1 Amplitude of the shear stress Π_m on the oscillating surface versus rarefaction parameter δ

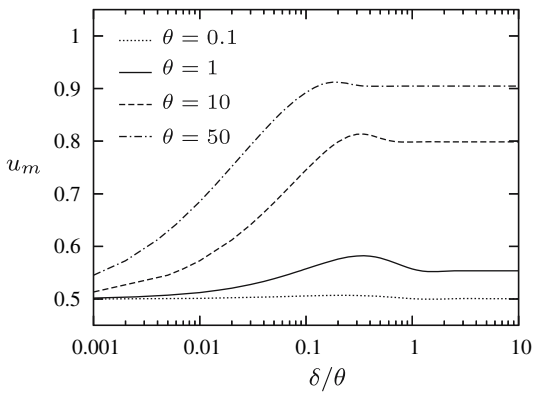

Fig. 2 Amplitude of the bulk velocity u_m on the oscillating surface versus rarefaction parameter δ

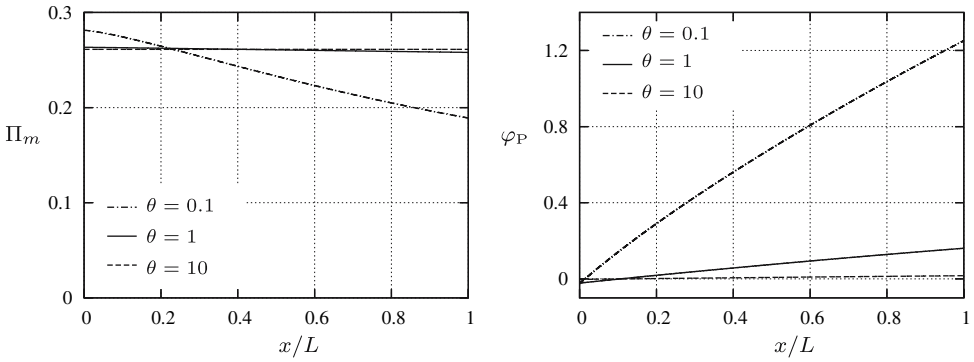

Fig. 3 Amplitude Π_m and phase φ_P of the shear stress versus distance x at $\delta = 0.1$

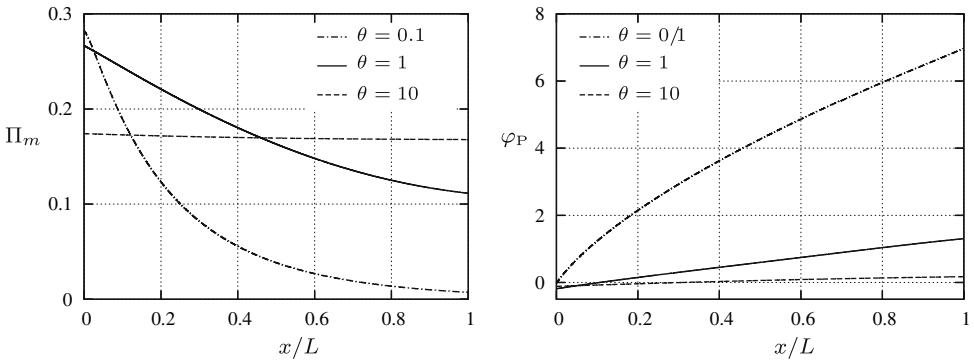

Fig. 4 Amplitude Π_m and phase φ_P of the shear stress versus distance x at $\delta = 1$

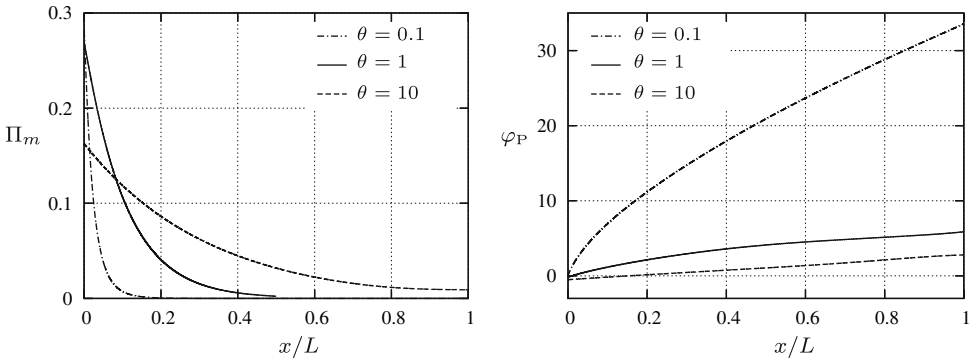

Fig. 5 Amplitude Π_m and phase φ_P of the shear stress versus distance x at $\delta = 10$

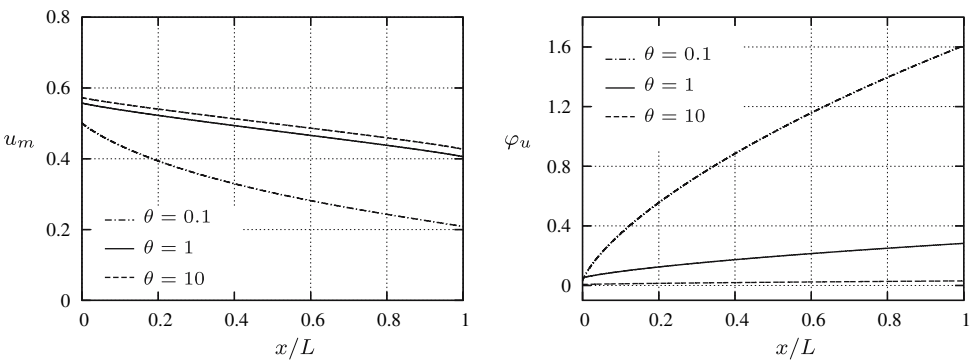

Fig. 6 Amplitude u_m and phase φ_u of the bulk velocity versus distance x at $\delta = 0.1$

velocity and shear stress were obtained in the free-molecular and slip regimes. It was shown that the use the free-molecular expression for the velocity and shear stress at the oscillating plate is justified if at least one of the two conditions $\delta = 0$ and $\theta = 0$ is satisfied. However, to apply the solution based on the Navier–Stokes equation with the

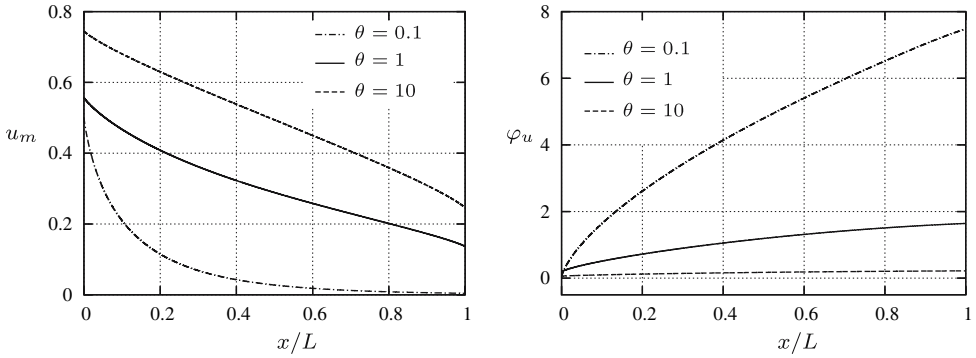

Fig. 7 Amplitude u_m and phase φ_u of the bulk velocity versus distance x at $\delta = 1$

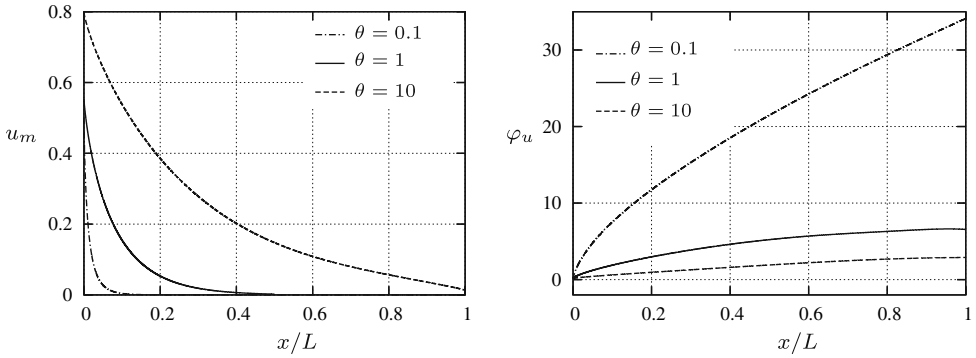

Fig. 8 Amplitude u_m and phase φ_u of the bulk velocity versus distance x at $\delta = 10$

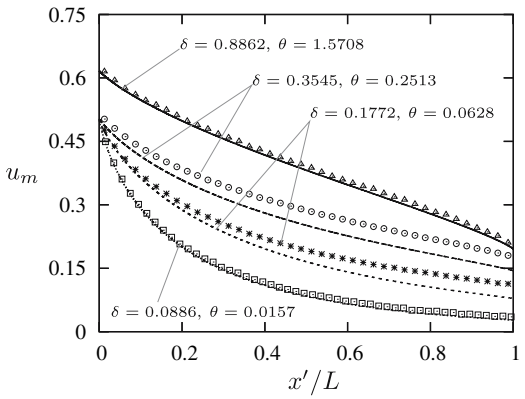

Fig. 9 Comparison with Park et al. (2004) *lines* present work, *symbols* Fig. 5a in Park et al. (2004)

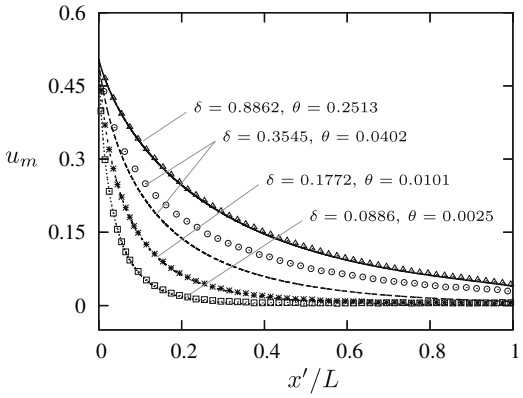

Fig. 10 Comparison with Park et al. (2004): *lines* present work, *symbols* Fig. 5b in Park et al. (2004)

slip boundary condition it is necessary to satisfy both conditions $\delta \gg 1$ and $\theta \gg 1$ simultaneously. If at least one of these parameters is not large, the problem is solved on the basis of the kinetic equation. The slip solution works well under these conditions if the rigorously obtained slip coefficient is used. The amplitude of the shear stress plotted versus the rarefaction parameter δ when the oscillation speed parameter is fixed has a minimum in the interval $0.1\theta \leq \delta \leq \theta$, while the bulk velocity has a maximum at the same point.

Acknowledgments The authors acknowledge the Conselho Nacional de Desenvolvimento Científico e Tecnológico (CNPq, Brazil) for the support of their research. Professor Dimitris Valougeorgis is acknowledged for the helpful discussion concerning the acceleration scheme. The authors also thank Professor Ali Beskok, who provided his numerical data to perform the precise comparison.

References

Abramowitz M, Stegun IA (eds) (1972) Handbook of mathematical functions with formulas, graphs and mathematical tables, 9 edn. Dover, New York

Bhatnagar PL, Gross EP, Krook MA (1954) A model for collision processes in gases. Phys Rev 94:511–525

Cercignani C, Pagani CD (1966) Variational approach to boundary value problems in kinetic theory. Phys Fluids 9(6):1167–1173

Gross EP, Ziering S (1958) Kinetic theory of linear shear flow. Phys Fluids 1(3):215–224

Hadjiconstantinou NG (2005) Oscillatory shear-driven gas flows in the transition and free-molecular flow regimes. Phys Fluids 17(100):611–619

Landau LD, Lifshitz EM (1989) Fluid mechanics. Pergamon, New York

Loyalka SK, Petrellis N, Storvik TS (1979) Some exact numerical results for the BGK model: Couette, Poiseuille and thermal creep flow between parallel plates. Z Angew Math Phys (ZAMP) 30:514–521

Marques Jr W, Kremer GM, Sharipov FM (2000) Couette flow with slip and jump boundary conditions. Continuum Mech Thermodyn 16(6):379–386

Naris S, Valougeorgis D (2005) The driven cavity flow over the whole range of the Knudsen number. Phys Fluids 17(9):097–106

Park JH, Bahukudumbi P, Beskok A (2004) Rarefaction effects on shear driven oscillatory gas flows: a direct simulation Monte Carlo study in the entire Knudsen regime. Phys Fluids 16(2):317–330

Sharipov F (2003) Application of the Cercignani–Lampis scattering kernel to calculations of rarefied gas flows. II. Slip and jump coefficients. Eur J Mech B Fluids 22:133–143

Sharipov F, Kalempa D (2003) Velocity slip and temperature jump coefficients for gaseous mixtures. I. Viscous slip coefficient. Phys Fluids 15(6):1800–1806

Sharipov F, Kalempa D (2007) Gas flow near a plate oscillating longitudinally with an arbitrary frequency. Phys Fluids 19(1):017–110

Sharipov F, Seleznev V (1998) Data on internal rarefied gas flows. J Phys Chem Ref Data 27(3):657–706

Sharipov F, Marques Jr W, Kremer GM (2002) Free molecular sound propagation. J Acoust Soc Am 112(2):395–401

Sharipov F, Cumin LMG, Kalempa D (2004) Plane Couette flow of binary gaseous mixture in the whole range of the Knudsen number. Eur J Mech B Fluids 23:899–906

Siewert CE (2002) Poiseuille, thermal creep and Couette flow: results based on the CES model for the linearized Boltzmann equation. Eur J Mech B Fluids 21:579–597

Siewert CE, Sharipov F (2002) Model equations in rarefied gas dynamics: viscous-slip and thermal-slip coefficients. Phys Fluids 14(12):4123–4129

Sone Y, Takata S, Ohwada T (1990) Numerical analysis of the plane Couette flow of a rarefied gas on the basis of the linearized Boltzmann equation for hard-sphere molecules. Eur J Mech B Fluids 9(3):273–288

Valougeorgis D, Naris S (2003) Acceleration schemes of the discrete velocity method: gaseous flows in rectangular microchannels. SIAM J Sci Comp 25(2):534–552

Willis DR (1962) Comparison of kinetic theory analyses of linearized Coutte flow. Phys Fluids 5:127–135